

Analysis of Two-dimensional Inflow Measurements by Lidar-Based Wind Scanners

AR. Meyer Forsting^{#1}, N. Troldborg[#], A. Sathe[#], N. Angelou[#]

[#]Department of Wind Energy, Technical University of Denmark

Frederiksborgvej 399, Risø Campus, 4000 Roskilde, Denmark

¹alf@dtu.dk

Keywords – Lidar, Induction, Inflow, Blockage, WindScanner, Data Processing, Modelling

The DTU led UniTTe project (unitte.dk) wants to establish lidars for power and load estimations for modern wind turbines. As these novel methods rely on scanning the flow upstream of the turbine, they come under the influence of the turbine induction zone [2], which develops due to the pressure jump induced by the turbine. Modeling and understanding the induction zone is key to establishing lidars as an industry standard for power and load estimations. Successfully modelling the upstream effects of the turbine, though, necessitates validation via measurements. The in-house developed short-range WindScanner system (windscanner.eu) is able to capture the entire wind field upstream by combining three synchronised lidars [1] and thus presents the ideal measurement tool for validating numerical models or other lidar systems.

This paper presents the challenges and methods in post-processing two-dimensional wind fields acquired by WindScanner like lidar systems for model validation purposes.

I. EXPERIMENTAL METHOD

The short-range WindScanner is based on three synchronised continuous wave Doppler lidars. They estimate the mean line of sight wind speed from the frequency shift in the laser Doppler spectra, resulting from moving airborne particles. The three lidars are synchronised such that their focal points are coinciding. The horizontal and vertical measurement grids were continuously scanned for 30 minutes. Both grids were fixed and thus only aligned with the turbine for one single wind direction. The horizontal plane was located at hub height and spanned the entire diameter (41 m) of the Risø NTK 500 turbine, as well as 62 m upstream. The vertical plane was perpendicular to the horizontal plane and had the same dimensions again spanning the entire rotor. One scan was completed in 15 s for the horizontal and 30 s for the vertical plane. Over three month a total of 32.5 h of data were acquired.

II. POST-PROCESSING

In this work the focus lies on post-processing of the line of sight velocities. There are many steps involved in the processing of the velocities such that they can be interpreted sensibly and finally be applied in the validation of a model (see Fig. 1).

A. Comparison with sonic anemometer and synchronisation

The first step is to find and remove spikes in the data. For this purpose firstly the despiking algorithm by Goring and Nikora [3] was used. To assess the measurement quality of the despiked data, the lidar velocities were compared to those acquired by a sonic anemometer that was situated on a short met mast inside the measurement grid. The correlation of these measurements was overall very satisfying, though it emerged that there was a random time shift between the two signals.

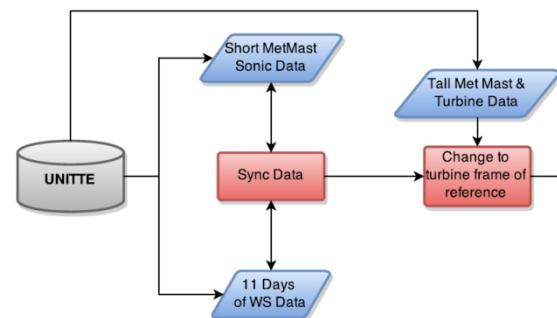


Fig. 1 Overview of the post-processing steps.

The time shift was estimated for all time series and applied to the measured data. Syncing allowed rejecting data for times when the turbine was barely running and enabled transforming it into the turbine frame of reference via the turbine's yaw data.

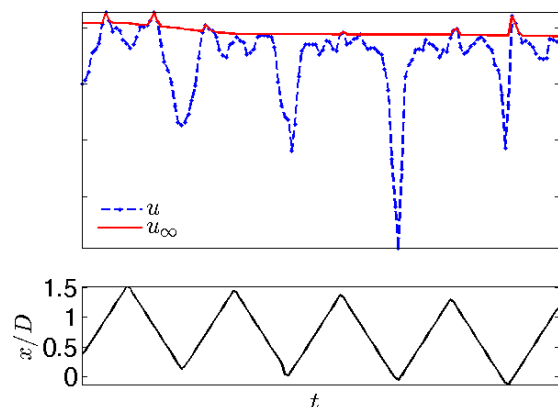


Fig. 2 Example of streamwise velocity component time series (u) and inlet velocity (u_∞) for a single scan. D represents the diameter of the turbine.

B. Despiking

The induction zone induces periodic dips in the streamwise velocity component (u) as the focal point of the three lidars approaches the turbine as shown in Fig. 2. These deep troughs caused the previously used spike detection algorithm to reject more than 20 % of the data. Therefore a novel gradient based spike detection tool was developed. Sorting the gradients from largest to smallest a logarithmic decay was observed to set in after about the first hundred points. All gradients lying inside this logarithmic region were assumed to be without spikes, gradients exceeding this threshold were tested for various spike conditions to determine their extent. Some examples are shown in Fig.3. This method did not remove all spikes, such that a visual inspection of the data became necessary. Only 1 in 1000 points was identified as abnormal by the user. This method only highlighted $> 2\%$ of the data as spikes.

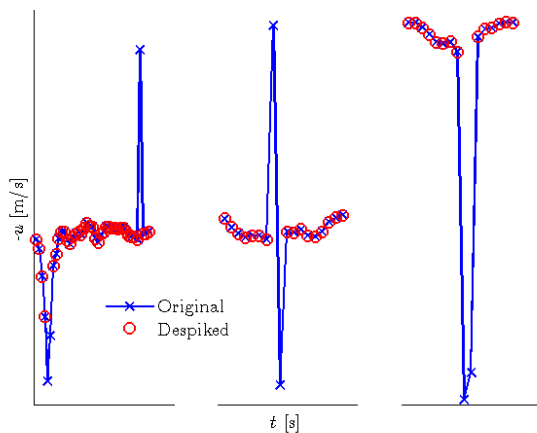


Fig. 3 Examples of successfully removed spikes.

C. Inlet velocity estimation

Consequently sorting the data by some measured parameter proved to be difficult. A tall met mast located closely to the WindScanner measurement grid showed strong decorrelation with the lidar data. The sonic met mast on the other hand was already under the influence of the turbine blockage. Not surprisingly it could be concluded that a point measurement was not sufficient to characterise the wind speed over a 2-D space. Therefore the lidar velocities themselves were taken to group the data. The streamwise component, u , is the most dominant and thus best suited for this purpose. The data points furthest from the turbine were expected to be least affected by the turbine blockage and expected to represent the free wind speed best. There were five maxima in x for each scan, but taking the average of the u component at these locations would have yielded an unsatisfactory result due to the large aleatory uncertainty of the wind speed over the scan periods. Instead points close to the maxima were incorporated by a weighting function. Furthermore it was checked if any maxima in u existed close to the most extreme x locations. Their value in combination with that resulting from the weighting function made up the stencils for the interpolation of the inlet velocity (u_∞). An example of this inlet velocity time series is shown in Fig. 2. Consequently each data point has its own individual inlet velocity.

D. Sorting horizontal data

Transforming the lidar data into the turbine frame of reference resulted into non-accessible clouds of free floating point data.

For the horizontal scans a mesh with the same resolution as that of the WindScanner grid of $4\text{m} \times 4\text{m}$ was established. The floating points can subsequently be averaged over a grid cell depending on the inlet velocity range to be analysed. A possible solution is shown in Fig.5.

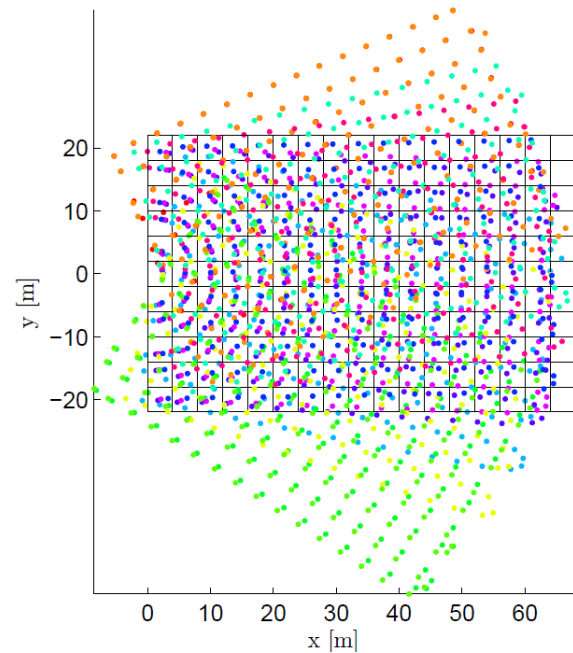


Fig. 4 Resampling the floating points of 8 scans.

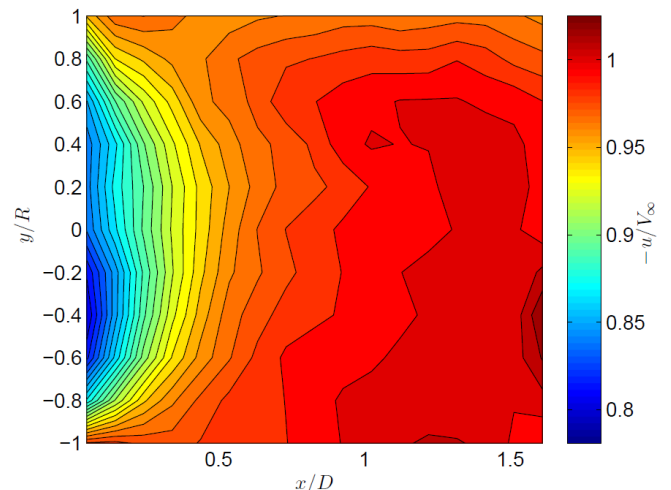


Fig. 5 Contours for $-u/V_\infty$ for inlet velocities $9.6 < u_\infty < 10.2$ m/s

E. Sorting vertical data

An equal procedure was used for the vertical scans, only that here the grid is polar, such that the points are sorted by the angle to the turbine centreline and grid location. Furthermore it was chosen to use the tall met mast velocity vector at hub height to sort the data instead of the inlet velocity, due to the atmospheric boundary layer affecting the

inlet velocity with height. An illustration of a potential solution is shown in Fig. 6.

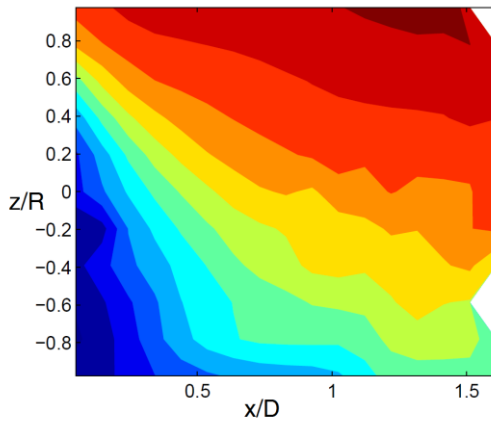


Fig. 6 Contours of $-u$ for $10.0 < V_{met} < 12.0$ m/s and $0^\circ < \theta < 5^\circ$.
Linear colour range from 8.5 m/s (blue) to 10.6 m/s (red).

III. CONCLUSION

The WindScanner system can characterise large wind fields remotely, potentially allowing the validation of numerical models over the entire domain of interest. Nevertheless multiple robust post-processing methods have to be applied to the lidar measurements to produce meaningful results. Especially spike detection and the aleatory uncertainty of wind speed require special attention when comparing the lidar data to other measurement techniques or numerical models.

ACKNOWLEDGEMENTS

This work was financed by The Innovation Fund Denmark, grant number 1305-00024B.

REFERENCES

- [1] Mikkelsen T., "Lidar-based Research and Innovation at DTU Wind Energy", Journal of Physics: Conference Series (Online), Vol.524, No. 1, 012007, 2014.
- [2] Medici D., Ivanell S., Dahlberg J.-Å., Alfredsson PH., "The upstream flow of a wind turbine: blockage effect", Wind Energy, Vol.14 pp. 691-697, 2011
- [3] Goring DG., Nikora VI., "Despiking acoustic doppler velocimeter data", Journal of Hydraulic Engineering, Vol. 128 pp. 117-126, 2002.